de Haas–van Alphen study of the charge-transfer salt α-(BEDT-TTF)$_2$KHg(SCN)$_4$ in pulsed magnetic fields of up to 54 T

N. Harrison
Laboratorium voor Vaste-Stoffysica en Magnetisme, Katholieke Universiteit Leuven, Celestijnenlaan 200D, B-3001 Heverlee, Belgium

A. House
Physics Department, University of Oxford, Clarendon Laboratory, Parks Road, Oxford OX1 3PU, United Kingdom

I. Deckers
Labortorium voor Vaste-Stoffysica en Magnetisme, Katholieke Universiteit Leuven, Celestijnenlaan 200D, B-3001 Heverlee, Belgium

J. Caulfield and J. Singleton
Physics Department, University of Oxford, Clarendon Laboratory, Parks Road, Oxford OX1 3PU, United Kingdom

F. Herlach
Laboratorium voor Vaste-Stoffysica en Magnetisme, Katholieke Universiteit Leuven, Celestijnenlaan 200D, B-3001 Heverlee, Belgium

W. Hayes
Physics Department, University of Oxford, Clarendon Laboratory, Parks Road, Oxford OX1 3PU, United Kingdom

M. Kurmoo
Physics Department, University of Oxford, Clarendon Laboratory, Parks Road, Oxford OX1 3PU, United Kingdom and The Royal Institution, 21 Albermarle Street, London W1X 4BS, United Kingdom

P. Day
The Royal Institution, 21 Albermarle Street, London W1X 4BS, United Kingdom

(Received 18 April 1995)

The de Haas–van Alphen effect has been measured in the organic conductor α-(BEDT-TTF)$_2$KHg(SCN)$_4$ in pulsed magnetic fields of up to 54 T, temperatures down to 350 mK, and at three different angles. Analysis of the amplitude of the quantum oscillations within the framework of a two-dimensional Lifshitz-Kosevich model reveals that this material appears to be only fully transformed into the high-field state at fields above $\sim$27 T, where the quasiparticle scattering rate is observed to be low. On entering the low-field state, the scattering rate is observed to increase dramatically. We also observe an apparent increase in the effective mass from $\sim 1.5m_e$ in the low-field state to $\sim 2.7m_e$ in the high-field state. The data at low fields are in accord with previous studies, but the nature of the higher harmonics of the de Haas–van Alphen oscillations at high fields appears to signify a departure from conventional Lifshitz-Kosevich behavior.

I. INTRODUCTION

Charge-transfer salts of the form (BEDT-TTF)$_n X$, where BEDT-TTF is bis(ethylenedithio)tetrathiafulvalene, have been the subject of intensive study, as they exhibit a wide variety of ground states and phases determined by the choice of anion X.[1] Amongst this family of materials, the series of salts α-(BEDT-TTF)$_2M$Hg(NCS)$_4$, where M=NH$_4$, K, Rb, or Tl, have proved especially interesting.[2–7] Although all possess very similar calculated Fermi surfaces consisting of an open quasi-one-dimensional (Q1D) electron section and a closed Q2D hole pocket, subtle differences in the nesting properties of the Q1D sections have a profound effect on their behaviors at low temperatures.[3–6] Whilst the salt with M=NH$_4$ is a superconductor below 1 K, those with M=K, Tl, or Rb exhibit what are thought to be spin-density wave (SDW) ground states at low temperatures.[3–7] One of the most noticeable features of the complex magnetic phase diagrams of the M=K, Rb, and Tl salts is observed as a sharp kink in the magnetoresistance;[3–6] it has become known as the "kink transition." The kink occurs at around 23 T in the M=K salt, and a number of authors have proposed that it represents destruction of the SDW ground state.[3–6] The reconstruction of the Fermi surface topology on passing through the kink has been studied extensively by Shubnikov–de Haas (SdH),[3–6] de Haas–van Alphen (dHvA),[8,9] and angle-dependent magnetoresistance oscillation (AMRO) measurements;[4,6] these studies were almost exclusively carried out using resistive or hybrid magnets, limiting the highest field to around 30 T. Below the kink, in the anti-

0163-1829/95/52(8)/5584(8)/$06.00

ferromagnetic regime, the quantum oscillations, attributed to the Q2D hole pocket, exhibit a very strong second harmonic (alternatively, one might say a very suppressed first harmonic), with the harmonic ratio showing a significant field dependence.[4,9] Above the kink, the quantum oscillation amplitude (at least of the first harmonic) increases dramatically.[3–5,8,9]

In the present experiments pulsed magnetic fields of up to 54 T have been employed to measure the dHvA effect in α-(BEDT-TTF)$_2$KHg(SCN)$_4$, both in the SDW regime and much deeper into the high-field state. The measurements complement previous pulsed-field SdH studies above the kink transition,[4,10] and enable the behavior of the quantum oscillations in the high-field state to be examined in a much less ambiguous way. Whereas the exact amplitude analysis of SdH oscillations is always complicated by the temperature and field dependence of the background magnetoresistance,[4,11] the amplitude of dHvA oscillations can be measured directly without the need for corrections.

II. EXPERIMENTAL DETAILS

Single-crystal α-(BEDT-TTF)$_2$KHg(SCN)$_4$ samples were grown using standard electrochemical techniques;[4] the resultant platelets had dimensions $\sim 1\times 1\times 0.2$ mm^3. Magnetic-field pulses of up to 54 T, in the form of a single, distorted half sine wave of duration 10–20 ms, were produced at the University of Leuven.[12] The dHvA detection coil was wound from 16-μm copper wire, with the compensation coil wound coaxially around it in opposite series configuration; with approximately 1000 turns, it was possible to compensate the pair of coils to better than 0.03%. A single crystal was placed on the end of the detection coils, which were dc coupled to an amplifier with a gain of 2500 and a bandwidth of $\sim$200 kHz. The cryostat was mechanically decoupled from the pulsed magnet and pumping systems, with additional vibration isolation provided between the ^{4}He cryostat and the plastic ^{3}He insert. Temperatures of $\sim$350 mK could be reached with no significant evaporation or temperature rise of the liquid ^{3}He occurring during or after a pulse.

III. de HAAS–van ALPHEN OSCILLATIONS

A. General features and oscillation frequencies

Figure 1 shows a typical dHvA signal from a single crystal of α-(BEDT-TTF)$_2$KHg(SCN)$_4$ as measured by a transient recorder connected to the amplifier output, with no background subtraction. The data were recorded on the rising side of the field pulse as the lower noise levels and higher (dB/dt) produce a better signal-to-noise ratio. The noise content was smaller at lower fields, allowing the oscillations below the kink (at $\sim$23 T) to be clearly resolved. The noise increased towards peak field, largely due to a contribution from copper-belly dHvA oscillations[11] originating from the polycrystalline copper of the detection coils [Fig. 1(b)]. Fourier transforms of the dHvA signals above and below the kink are shown in Fig. 2(a); the data sets were modulated by Hanning windows.[11] At fields above the kink, the strong harmonic

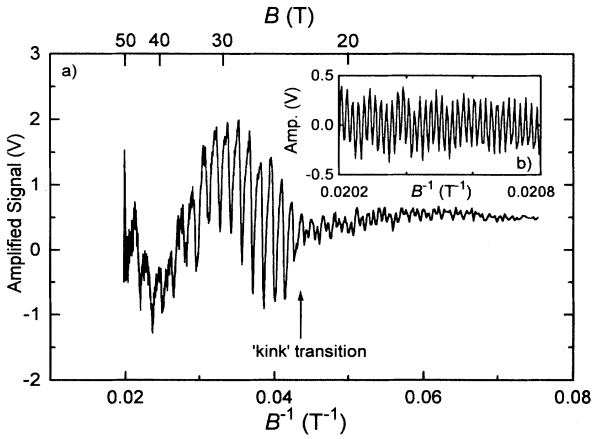

FIG. 1. (a) An example of raw de Haas–van Alphen signal plotted as amplified detection coil voltage (i.e., amplifier output) vs inverse field. No background subtraction has been applied to the data, and the temperature during this experiment was 350 mK. (b) An example of quantum oscillations from the polycrystalline copper comprising the dHvA detection coils, detected at the highest magnetic fields. This observation is indicative of the high sensitivity of the dHvA apparatus.

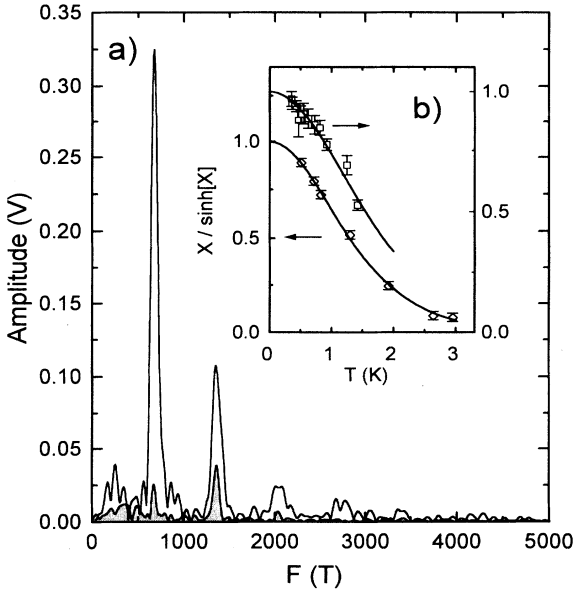

FIG. 2. (a) Fourier transforms of the data in Fig. 1(a) carried out both above (unshaded) and below (shaded) the kink transition. (b) The temperature dependence of the first-harmonic amplitude at $\sim$29 T (i.e., above the kink) obtained by Fourier analysis of the dHvA data in this work (square symbols). A fit to the R_T factor $X/\sinh[X]$ (solid line; see text) gives an effective mass of $\sim 2.7 m_e$. The reanalyzed amplitudes of the SdH data at $\sim$24 T of Ref. 4 are shown as diamond symbols for comparison; the fitted curve also gives an effective mass of $\sim 2.7 m_e$. All of the amplitudes are renormalized to 1.

content is particularly striking, with harmonics up to the fifth present. Below the kink, the first harmonic is strongly reduced in amplitude relative to the second; this is in accord with other dHvA and SdH measurements made below the kink.[3–5,8,9,13] Both above and below the kink the frequency F of the dHvA oscillations was found to be 670±3 T.

A number of authors have recently noted quantum oscillations of a frequency around 4300 T below the kink in α-(BEDT-TTF)$_2M$Hg(SCN)$_4$, with M=K and Tl, both in SdH (Refs. 3 and 4) and dHvA (Ref. 13) experiments. This frequency has been attributed by some[3] to a breakdown orbit involving the whole un-nested Fermi surface; this contention has then been used to argue that the state below the kink is a mixture of "normal metal" and SDW phases. Given the amplitude of the 4300-T oscillations at fields below the kink[3,4,13] and the signal-to-noise ratio of the dHvA system in this work, these high-frequency oscillations should be observable in our data above 30 T. However, at the very highest fields, the only rapid oscillations in fact observed are due to the 60-kT copper-belly frequency[11] [Fig. 1(b)]. This implies that the 4300-T frequency discussed in Refs. 3, 4, and 13 arises from the SDW state present below the kink, rather than a breakdown orbit of the un-nested Fermi surface.

B. de Haas–van Alphen effect due to a 2D Fermi surface

The Fermi surface of α-(BEDT-TTF)$_2$KHg(SCN)$_4$, prior to the formation of the SDW, is known to consist of Q1D and Q2D components.[3–6] Only the closed Q2D portion of the Fermi surface appears to contribute to the dHvA above the kink, giving the observed F=670 T frequency.[3–6,8,9,13] In 3D k space, the Q2D component is better described as a weakly corrugated cylinder centered on the corner of the Brillouin zone.[3–6] In conventional 3D systems, the phase smearing due to local curvature of the Fermi surface about each extremal dHvA orbit is found by integrating over the frequency contributions to the quantum oscillations as a function of k_z (i.e., parallel to B).[11] In the 3D Lifshitz-Kosevich (LK) model for the dHvA effect, the integration limits are approximated to $-\infty < k_z < \infty$. In the case where $\Delta F/2B < 1$, however, these integration limits are no longer appropriate and a finite integration between $\pm K_b/2$ must be performed (K_b is the component of the reciprocal lattice vector in the direction of B). Given that no dHvA beats are observed in α-(BEDT-TTF)$_2$KHg(SCN)$_4$ over the entire field range (see also Refs. 3–5, 8, and 9), we can assume that we are in the limit where $\Delta F/2B \ll 1$. Hence, a correct analysis of the quantum oscillations calls for the normal 3D LK theory to be replaced by an equivalent 2D treatment.

The oscillatory magnetic moment for a 2D Fermi surface may be derived from the semiclassical expression for the chemical potential of a 2D slab of k space given in Chap. 2 of Ref. 11, with the assumption that F is invariant over k_z. It is expected that the amplitude reduction factors for thermal-broadening effects (R_T), the effects of a finite relaxation time (R_D), and the phase mixing between the spin-up and spin-down channels (R_S) will be the same as in the 3D case [see e.g., Eqs. (2.128), (2.137), and (2.148) of Ref. 11]. Remembering that the signal in a pulsed-field dHvA experiment is measured as an induced voltage V in the detection coils, some manipulation yields

$$V=\sum_p \alpha(p,B,T)\cos\left[2\pi\left[\frac{F}{B}-\frac{1}{2}\right]\right], \tag{1}$$

with

$$\alpha(p,B,T)=2p\eta\Omega k_B K_b (F^2/B^3)\frac{dB}{dt}\frac{e}{\hbar}\frac{T}{\sinh X}R_D R_S . \tag{2}$$

Here p denotes the harmonic number $X=(2\pi^2 p k_B T)/(\hbar\omega_c)$, $\omega_c=eB/m^*$ is the effective cyclotron frequency, m^* is the quasiparticle effective mass, Ω is the sample volume, and η is the geometric coupling factor of the sample to the detection coils. Note that (dB/dt) varies throughout the pulse; this variation is recorded in the experiments and is always implicitly included in our analysis of the results.

There are differences between Eq. (1) and the 3D LK expression[11] that affect the analysis of the quantum oscillations. Firstly, there is no $\pi/4$ phase component in the oscillatory factor, and, secondly, the exponent of the magnetic field B is 3 instead of $\frac{5}{2}$. Estimates of the quasiparticle scattering rate τ^{-1}, the g factor, the absolute amplitude of the quantum oscillations, and the harmonic ratios will also differ from those obtained using 3D analysis. Nevertheless, the procedure for determining m^* by fitting the oscillation amplitude as a function of temperature to the term $R_T=X/\sinh X$ is still the same,[11] whether the 2D or 3D LK model is assumed.

C. The effective masses

Fits of the dHvA oscillation amplitude to R_T (as constant B) provide the best estimate of the effective mass, since the expression has a distinct functional form derived from the Fermi-Dirac distribution function.[11] By convention,[11] the argument of the hyperbolic sine term is approximated to $X\cong 14.69(m_p^*/m_e)(T/B)$ (where m_e is the free-electron mass). This ignores the harmonic index p, so that the fitted mass m_p^* of the pth harmonic is higher by a factor p than the actual mass. In our analysis, all amplitudes of the quantum oscillations were obtained by Fourier analysis over short intervals of reciprocal-field space with the short data sets modulated by Hanning windows. A typical fit is shown in Fig. 2(b).

There is controversy surrounding the quoted values, derivation, and possible field dependence of the effective mass in this material.[3–5,8,9,13] There have been reports of a difference between the effective mass determined at fields below the kink from SdH data and that determined from dHvA experiments.[4,13] The reason for this is unclear, but an explanation may be connected with the strong temperature dependence of the background magnetoresistance observed below the kink.[4] Values of m_p^* determined from the pulsed-field dHvA oscillations are shown in Fig. 3(a), along with values obtained from conventional field-modulation dHvA measurements below

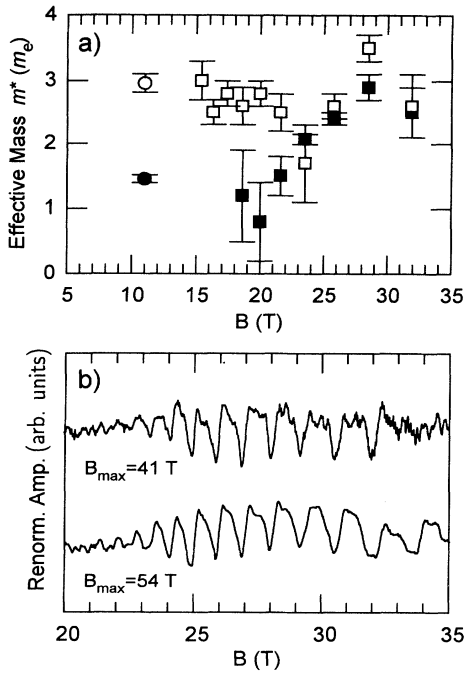

FIG. 3. (a) The derived effective masses of the first harmonic (filled symbols) and second harmonic (open symbols) plotted as a function of magnetic field. The values obtained in static magnetic field dHvA experiments (Ref. 13) below the kink are indicated by circular symbols. (b) Examples of dHvA oscillations (renormalized to take into account dB/dt), for field pulse heights of 41 and 54 T. The 54-T pulse had double the rate of change of magnetic field dB/dt and therefore approximately quadruple the heat input of the 41-T pulse. This clearly demonstrates that heating of the sample was not a significant factor in our experiments, although the signal-to-noise ratio of the data from the 41-T pulse is slightly worse. The temperature was the same ($\sim$570 mK) for both pulses.

the kink.[13] The estimates made for the mass of the first harmonic m_1^* below the kink from our experiments have a greater error due to their relatively low amplitude compared to the oscillations above the kink; nevertheless, the masses obtained below the kink in this work are consistent with the values derived by other authors, which range from $1.4-1.9m_e$.[3–5,8,9,13]

An apparent increase in m_1^* is observed as the magnetic field drives the sample through the kink transition. The average effective mass for the entire field region above the kink was estimated to be $2.7\pm0.1m_e$. These results contradict earlier works in which the mass was reported to be the same above and below the kink.[4,9] In the case of Ref. 4, this conclusion was based on SdH measurements made in a hybrid magnet in fields up to 25 T. Estimates of the effective mass depend somewhat on the technique used to determine the amplitude of the quantum oscillations. In Ref. 4 the amplitude above the kink was taken as the peak-peak size of the oscillations. Owing to the presence of a strong harmonic content in the signal, this method is less reliable than the Fourier technique in this work. The results of the application of Fourier analysis techniques to the SdH data recorded above the kink in Ref. 4 are also shown in Fig. 2(b), yielding $m_1^*=2.75\pm0.05m_e$, in comfortable agreement with the dHvA results in this work.

At fields below the kink, the second harmonic mass was found to be $m_2^*=2.7\pm0.2m_e$ using Fourier analysis of the dHvA data over the field range 15–22 T. This is around double that of the first harmonic over the same field range, and is therefore consistent with the LK model, implying normal Fermi-liquid behavior.[11] At fields above the kink, however, $m_2^*=3.0\pm0.2m_e$, instead of the expected $5.4m_e$. Our reanalysis of the SdH data in Ref. 4 yielded $m_2^*=2.6\pm0.4m_e$ above the kink, also lower than the expected value and in agreement with the dHvA result in this work. The mass of the third harmonic from the dHvA data was found to be similar above the kink, at $m_3^*=2.7\pm0.6m_e$. The similar estimated harmonic masses above the kink suggest a strong departure from normal LK behavior. The effective masses of the fourth and higher harmonics could not be determined with any accuracy.

Strong harmonic content and other anomalous behavior could be caused by the Shoenberg magnetic interaction.[11,14] For this effect to be important, the oscillatory magnetization $M=m/V$ of the sample must approach (or exceed) the field interval B^2/F between successive quantum oscillations. Using Eqs. (1) and (2) to estimate the maximum possible amplitude of the quantum oscillations in the absence of all phase smearing effects, and setting $m_1^*=2.7m_e$ (this work) and $K_b=3.1\times10^9$ m^{-1} (Refs. 3–5) yields $M\sim200$ A m^{-1}; this corresponds to an oscillatory field inside the sample of 0.3×10^{-4} T. Given that this is much smaller than B^2/F, we can rule out the involvement of the Shoenberg magnetic interaction.

Eddy-current heating of the sample might be a possible cause of anomalous mass estimates, especially since previous SdH measurements in pulsed fields have suggested this effect.[10] The power dissipated by eddy currents within the sample is roughly proportional to $(dB/dt)^2$, and so to check whether heating was a problem different rates of change of magnetic field were applied to the sample by changing the field pulse height.[12] Figure 3(b) shows the result of increasing the pulse height from 40 to 54 T, thereby doubling (dB/dt) and roughly quadrupling the heat input; data are normalized to take into account the different values of (dB/dt). No significant difference in oscillation amplitude is observed, indicating that heating is not an important factor in spite of the poor thermal conductivity of liquid ^{3}He; this was probably due to efficient heat-sinking of the sample to the detection coil.

D. Quasiparticle scattering effects and the absolute amplitude of the quantum oscillations

Figure 4(a) shows Dingle plots (i.e., $\ln[A]=\ln[\alpha_m(p,B,T)B^3\sinh[X]/(dB/dt)pT]$ versus $1/B$) for the measured amplitudes a_m of the first and second harmonics of the dHvA oscillations. Dingle plots from individual field pulses were found to be identical within

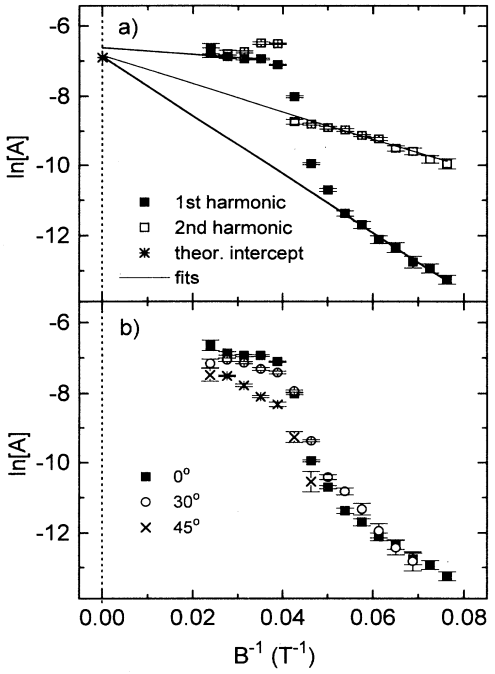

FIG. 4. (a) Plots of the logarithmic amplitude $\ln[A]$ of the dHvA oscillations (known as Dingle plots) for the first and second harmonics of the dHvA oscillations. Fits are made to the linear portions of the graph (above 27 T and below 20 T), with the results shown in Table I. In addition, the infinite field amplitude expected from theory, $\ln[A_0]$, is shown as a star. (b) Dingle plots for tilted-field dHvA experiments; the tilt angles are indicated in the figure.

the experimental error, and so the points in Fig. 4(a) were derived by averaging separate Dingle plots for twelve sets of experimental data recorded at temperatures between 0.35 and 1.5 K. This procedure also provides an estimate of the standard error. Furthermore, it should be pointed out that the field ranges (i.e., Hanning windows) used to derive each point in Fig. 4(a) do not overlap. From Eqs. (1) and (2), the gradient of such a Dingle plot should be $-pm^*\pi/e\tau \cong -14.69m^*T_D$, yielding the scattering rate and the Dingle temperature T_D. The intercept $\ln[A_0]$ of the graph at $1/B=0$ can be used to compare the measured amplitude with that expected from Eqs. (1) and (2). Constant masses of $2.7m_e$ for fields above the kink and $1.5m_e$ below the kink have been assumed for the first harmonic, except in the transition region near the kink where local mass estimates are more reliable. Likewise, for the second harmonic the constant mass estimates above and below the kink quoted above were used.

The Dingle plot of the first harmonic reproduces previous results[4,8,9] for fields up to 27 T. However, the present study also shows an additional shallow-sloped region above ~27 T, not previously reported due to the limited field available in earlier studies [Fig. 4(a)]. It appears from Fig. 4(a) that the fields above ~27 T correspond to the high-field state of α-(BEDT-TTF)$_2$KHg(SCN)$_4$, whereas those below ~20 T correspond to the low-field state. The region between is roughly centered on the kink transition (~23 T) and appears to represent a gradual transition between the two regimes (Refs. 4, 8, and 9). In contrast to the fairly gentle increase in amplitude in this region observed for the first harmonic, the second harmonic shows a more abrupt change. Above the kink, an anomalous positive slope of the second-harmonic Dingle plot is observed, which is inconsistent with the LK model and again draws attention to the unusual behavior of the quantum oscillations in high magnetic fields.

Linear fits (i.e., avoiding curved regions near the kink) were made to the Dingle plots of Fig. 4(a) and are summarized in Table I, which also shows a reanalysis of the 25-T hybrid magnet SdH data of Ref. 4 for comparison. In most cases the agreement between the results of the SdH and dHvA analysis is good; below the kink the masses implied by SdH and dHvA differ, but nevertheless the values of m^*T_D are in good agreement. This is not unexpected, as crystals used in both experiments were prepared using identical techniques.

Previous studies on α-(BEDT-TTF)$_2$KHg(SCN)$_4$ have shown that, below the kink, the first harmonic of the quantum oscillations is close to a "spin-zero", i.e., almost perfect phase cancellation between the spin-up and spin-

TABLE I. Experimental effective masses, Dingle temperatures, scattering rates, and logarithmic dHvA amplitudes at infinite field derived using the de Haas–van Alphen data (dHvA) in this work and the Shubnikov–de Haas results in Ref. 4 (SdH). The final column contains theoretical estimates of the logarithmic dHvA amplitudes at infinite field. "Low field" and "high field" indicate fields below 20 T and above 27 T, respectively.

Regime	Harmonic no.	Data	m^* (m_e)	m^*T_D (m_eK)	τ^{-1} ($\times 10^{12}$ s^{-1})	$\ln[A_0]$ (expt.)	$\ln[A_0]$ (theory)
	first	dHvA	1.5	5.7(4)	3.1(4)	−6.9(2)	−6.9
low		SdH	1.9	5.5(2)	2.3(1)		
field	second	dHvA	2.7	5.4(3)	1.6(1)	−6.8(2)	−6.9
		SdH	3.8	5.66(5)	1.2(1)		
	first	dHvA	2.7	0.6(4)	0.2(1)	−6.6(3)	−6.9
high		SdH	2.75				
field	second	dHvA	3.0				−6.9
		SdH	2.6				

down contributions to the quantum oscillations, causing the factor R_S to tend to zero.[3–5,8,9] This observation is reflected in our data by the strong reduction of the first harmonic below the kink compared to the second, as seen in Fig. 4(a). In addition, previous studies have suggested that the strong field dependence of the harmonic ratio implies that the R_S factor also changes with magnetic field;[4,5,9] this has been interpreted within the LK framework by assuming a field-dependent g.[4,5,9] This observation is also reflected in the present dHvA data and the SdH results of Ref. 4 by the disagreement between the estimates of τ^{-1} obtained for the first and second harmonics. If normal LK behavior is applied, then the scattering rates for the first and second harmonics should be identical. In this context it is worth mentioning that there is a difference by a factor of $\sqrt{2}$ between the harmonic ratios of the 3D and 2D LK models. This only results in small differences in the precise values of g obtained.

Nevertheless, if we choose to ignore the R_S factor, the infinite field intercepts of the Dingle fits are all found to be consistent with each other and are within a factor 2 of those expected from the 2D LK model [Table I, last column and Fig. 4(a)]. This is a satisfactory agreement, given the uncertainties in many experimental factors. For this calculation, the sample volume was measured to be $V \sim (1.6 \pm 0.1) \times 10^{-10}$ m^3, and the geometric coupling factor η was calibrated to be around 0.1 H m^{-1}. Possible sources of error are expected from our assumption of $R_S \sim 1$ for the spin-splitting factor, phase smearing of the quantum oscillations due to the weak corrugation of the Fermi surface, and probably also the field dependence of g or m^*, which may affect the slope of the Dingle plot. The close correlation between the infinite field intercepts above and below the kink and the fact that F is the same (within experimental error) above and below the kink suggest that the quantum oscillations detected in both regimes originate from similar pieces of Fermi surface. However, the quasiparticle scattering rate increases greatly from $\tau^{-1} \sim 2 \times 10^{11}$ s^{-1} above ~ 27 T to $\tau^{-1} \sim 2 \times 10^{12}$ s^{-1} below 20 T, indicating that additional quasiparticle scattering processes come into existence below the kink compared to the high-field state; these additional scattering processes are possibly associated with the formation of the SDW. This result contradicts the conclusions of previous studies based on experiments up to only ~ 30 T,[4,8,9] which suggested that the scattering rate increased above the kink. As we have seen, the limited field range of the earlier studies meant that only the extended transition region, and not the high-field state, was accessed.

IV. TILTED-FIELD de HAAS–van ALPHEN STUDIES

The crystal was remounted inside the dHvA detection coil with the crystallographic b axis at 30° and 45° to the applied magnetic field. As the crystal was rotated the overall amplitude of the quantum oscillations was observed to diminish, with the relative size of the second harmonic decreasing more strongly. For this reason, it was not possible to make a reliable estimate of the mass associated with the second harmonic at different angles. It was also not possible to make reliable mass estimates of the first harmonic below the kink, but above the kink the masses were observed to increase with angle as expected from the increase in the area of the dHvA orbit.[3–5]

Dingle plots of the first harmonic at 0°, 30°, and 45° are shown together in Fig. 4(b), with the results of fits to the Dingle plots shown in Table II together with the derived effective masses. The slopes of all the Dingle plots both above and below the kink are observed to increase. In the high-field state, the absolute amplitude intercept is observed to increase in accordance with that expected from simple LK theory. The derived scattering rate, on the other hand, is seen to increase strongly with angle. From a semiclassical viewpoint the scattering rate should be observed to marginally decrease with angle, due to the slower motion of the orbitally averaged heavier quasiparticles; the experimental result here may therefore indicate an anisotropic scattering mechanism. In spite of this observation, we continue to find at increasing angles that the scattering rate (at least at 30°) increases significantly on entering the low-field state below the kink.

V. DISCUSSION AND CONCLUSION

Strong de Haas–van Alphen oscillations have been observed in the organic conductor α-(BEDT-TTF)$_2$KHg(SCN)$_4$ in pulsed magnetic fields of up to 54 T, temperatures down to 350 mK, and at several different angles. The analysis of the amplitude of the quantum os-

TABLE II. The effect of tilting the magnetic field on the dHvA frequency, effective masses, Dingle temperatures, scattering rates, and logarithmic dHvA amplitudes at infinite field. The final column contains theoretical estimates of the logarithmic dHvA amplitudes at infinite field. "Low field" and "high field" indicate fields below 20 T and above 27 T, respectively.

Regime	Angle	Freq. (T)	m^* (m_e)	m^*T_D (m_eK)	τ^{-1} ($\times 10^{12}$ s^{-1})	ln[A_0] (expt.)	ln[A_0] (theory)
high	0°	670	2.7(1)	0.6(4)	0.2(1)	−6.6(3)	−6.9
field	30°	774	2.8(6)	2.0(3)	0.6(1)	−6.2(2)	−6.6
	45°	948	3.5(5)	5.0(3)	1.2(1)	−5.4(1)	−6.2
low	0°	670	1.5(3)	5.7(4)	3.1(2)	−6.9(2)	−6.9
field	30°	774	1.7	8.9(7)	4.3(3)	−3.8(5)	−6.6
	45°	948	2.1				−6.2

cillations indicates that α-(BEDT-TTF)$_2$KHg(SCN)$_4$ is only fully transformed into the high-field state for fields above $\sim$27 T. The strong increase in the amplitude of the quantum oscillations above 23 T noted in previous studies, and incorrectly interpreted as an increase in the Dingle temperature T_D of the sample at high fields,[4,8,9] in fact appears to correspond to an extended transition region between the low- and high-field states, centered roughly on the kink. The extended nature of the transition between low- and high-field states is also apparent in AMRO studies.[4,5]

Fourier analysis of the dHvA oscillations above and below the kink has revealed that the fundamental frequencies F are identical to within 0.3%. This suggests that the Q2D portion of the Fermi surface is virtually unaffected by the formation of the SDW. In the high-field state above $\sim$27 T, the slope of the Dingle plot is low, with $T_D \sim 0.2$ K, indicating good sample quality. However, the strong suppression of the dHvA oscillations below the kink indicates that the formation of the SDW is accompanied by a large increase in the quasiparticle scattering rate. The large quasiparticle scattering rate below the kink is observed in both the first and second harmonics. Such an effect might be expected if the SDW were to introduce some form of disorder in the system. The possible origin of this disorder might be the domain structure indicated by the well-documented hysteresis in the magnetoresistance.[3–6]

In the high-field state, where the SDW is destabilized, the fitted effective mass of the carriers increases by approximately a factor of 2. This increase perhaps signals an enhancement of the electron-electron or electron-phonon interactions above the kink. It is notable that the effective mass of the carriers in α-(BEDT-TTF)$_2$KHg(SCN)$_4$ measured at fields below the kink is anomalously low compared to those of isostructural salts such as α-(BEDT-TTF)$_2$NH$_4$Hg(SCN)$_4$ (Ref. 16) and α-(BEDT-TTF)$_2$TlHg(SeCN)$_4$ (Ref. 17), which do not exhibit a SDW ground state. The larger mass seen in the high-field state of α-(BEDT-TTF)$_2$KHg(SCN)$_4$ may therefore be a more representative value. The destruction of the SDW also brings about a reduction in the scattering rate, as mentioned above. The decrease in the scattering rate and the increase in the quasiparticle effective mass occur at about the same point of field, strongly suggesting that the two phenomena are connected.

In the high-field state the presence of strong higher harmonics, which possess lower than expected effective masses, suggests that, e.g., magnetic interaction effects might be affecting the dHvA waveform. However, both the theoretical and measured absolute amplitude estimates give a magnetization which is too small to cause conventional magnetic interaction. These and other aspects of the behavior of the high-field quantum oscillations in this and other very recent works[17] suggest that studies of the applicability of the LK formalism to Q2D organic metals as the quantum limit is approached are now necessary. The utility of the dHvA pick-up coil techniques reported in this work cannot be overemphasized in this context; in contrast to either SdH or torque dHvA measurements, the signal derived from the sample may be simply related in a quantitative manner to theoretical expressions for the density of states at the Fermi energy.

Note added in proof. Two recent works that in general support the conclusions of this paper have come to our notice. The first [P.S. Sandhu, G.J. Athas, J.S. Brooks, E.G. Haanappel, J.D. Goettee, D.W. Rickel, M. Tokumoto, N. Kinoshita, T. Kinoshita and Y. Tanaka (unpublished) concerns an experimental study of Shubnikov–de Haas oscillations in (BEDT-TTF)$_2$MHg(NCS)$_4$ (M=NH$_4$, Tl) at fields of up to 50 T. Deviations from Lifshitz-Kosevich behavior similar to those reported in this work are reported. The second (P. Christ, W. Biberacher, A.G.M. Janssen, M.V. Kartsovnik, A.E. Kovalev, N.D. Kusch, E. Steep, and K. Andres, *Proceedings of the 11th International Conference on the Electronic Properties of Two Dimensional Systems, Nottingham, UK, 1995* [Surf. Sci. (to be published)]) reports torque de Haas–van Alphen data up to 30 T for (BEDT-TTF)$_2$KHg(NCS)$_4$, which confirm the increase in effective mass above the kink reported in this paper.

ACKNOWLEDGMENTS

This work was supported by the National Fonds voor Wetenschappelijk Onderzoek (Belgium), the EPSRC (UK), and the European Community Human Capital and Mobility and Large Installations programs. N.H. is a postdoctoral fellow of the Onderzoeksraad KU Leuven. A.H. acknowledges the provision of an ERASMUS studentship. The contributions of Professor G. Pitsi and Professor C. Agosta in providing various parts of the ^{3}He system is acknowledged. We should like to thank Dr. S. Uji and Professor D. Shoenberg for stimulating discussions and access to data prior to publication.

---

[1]For a recent review, see Proceedings of the International Conference on Science and Technology of Synthetic Metals, Seoul, Korea, 1994 [Synth. Met. **69-71** (1995)].

[2]A very large body of literature now exists concerning these materials. In order to avoid unnecessary and extensive duplication, readers are referred to Refs. 3–7, which contain the most recent experimental results, thorough overviews of previous work, and comprehensive lists of earlier relevant papers.

[3]X. Chen, J. S. Brooks, S. J. Klepper, S. Valfells, G. J. Athas, Y. Tanaka, T. Kinoshita, N. Kinoshita, M. Tokumoto, H. Anzai, and C. C. Agosta (unpublished); S. Uji, T. Terashima, H. Aoki, J. S. Brooks, M. Tokumoto, N. Kinoshita, T. Kinoshita, Y. Tanaka, and H. Anzai, J. Phys. Condens. Matter **6**, L539 (1994); S. Uji, H. Aoki, J. S. Brooks, A. S. Perel, G. J. Athas, S. J. Klepper, C. C. Agosta, D. A. Howe, M. Tokumo-

to, N. Kinoshita, Y. Tanaka, and H. Anzai, Solid State Commun. **88**, 683 (1993).

[4]J. Caulfield, S. J. Blundell, M. S. L. du Croo de Jongh, P. T. J. Hendriks, J. Singleton, M. Doporto, F. L. Pratt, A. House, J. A. A. J. Perenboom, W. Hayes, M. Kurmoo, and P. Day, Phys. Rev. B **51**, 8325 (1995).

[5]T. Sasaki and N. Toyota, Phys. Rev. B **49**, 10 120 (1994).

[6]M. V. Kartsovnik, H. Ito, T. Ishiguro, H. Mori, T. Mori, G. Saito, and S. Tanaka, J. Phys. Condens. Matter **6**, L479 (1994); M. V. Kartsovnik, A. E. Kovalev, V. N. Laukhin, I. F. Schegolev, H. Ito, T. Ishiguro, N. D. Kusch, H. Mori, and G. Saito, in *Proceedings of the International Conference on Science and Technology of Synthetic Metals, Seoul, Korea, 1994* (Ref. 1), p. 811.

[7]F. L. Pratt, T. Sasaki, N. Toyota, and N. Nagamine, Phys. Rev. Lett. **74**, 3892 (1995).

[8]P. Christ, W. Biberacher, H. Muller, and K. Andres, Solid State Commun. **91**, 451 (1994); P. Christ, W. Biberacher, H. Müller, K. Andres, E. Steep, and A. G. M. Jansen, Physica B **204**, 153]

[9]T. Sasaki and N. Toyota, Synth. Met. **55-57**, 2296 (1993); T. Sasaki, Ph.D. thesis, Tohoku University, Sendai, 1992.

[10]John Singleton, Jason M. Caulfield, S. O. Hill, P. T. J. Hendriks, F. L. Pratt, M. Doporto, I. Deckers, G. Pitsi, F. Herlach, W. Hayes, T. J. B. M. Janssen, J. A. A. J. Perenboom, M. Kurmoo, and P. Day, in *Proceedings of Conference Physique en Champs Magnétiques Très Intenses et Technologies Associées, Toulouse, 1993,* edited by J. Leotin (CNRS-UPS-INSA, Toulouse, 1993), p. J2-1.

[11]D. Shoenberg, *Magnetic Oscillations in Metals* (Cambridge University Press, Cambridge, 1984).

[12]F. Herlach, M. van der Burgt, I. Deckers, G. Heremans, G. Pitsi, and L. van Bockstal, Physica B **63**, 177 (1992).

[13]C. Haworth, J. Caulfield, R. Corcoran, J. Singleton, S. Hayden, and M. Springford (unpublished).

[14]M. Doporto, J. Singleton, F. L. Pratt, J. Caulfield, W. Hayes, J. A. A. J. Perenboom, I. Deckers, G. Pitsi, M. Kurmoo, and P. Day, Phys. Rev. B **49**, 3949 (1994).

[15]J. Caulfield, J. Singleton, P. T. J. Hendriks, J. A. A. J. Perenboom, F. L. Pratt, M. Doporto, W. Hayes, M. Kurmoo, and P. Day, J. Phys. Condens. Matter **6**, L155 (1994).

[16]T. Osada, A. Kawasumi, R. Yagi, S. Kagoshima, N. Miura, M. Oshima, H. Mori, T. Nakamura, and G. Saito, Solid State Commun. **75**, 901 (1990); M. Doporto, F. L. Pratt, J. Singleton, M. Kurmoo, and W. Hayes, Phys. Rev. Lett. **69**, 991 (1992).

[17]V. N. Laukhin, A. Audouard, H. Rakoto, J. M. Broto, F. Goze, G. Coffee, L. Brossard, J. P. Redoules, M. V. Kartsovnik, N. D. Kusch, L. I. Buravov, A. G. Khomenko, E. B. Yagubskii, S. Askenazy, and P. Pari, Physica B **211**, 282 (1995).

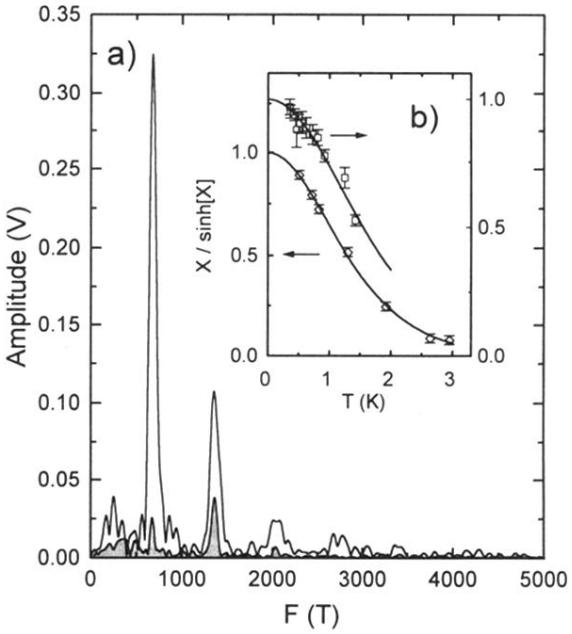

FIG. 2. (a) Fourier transforms of the data in Fig. 1(a) carried out both above (unshaded) and below (shaded) the kink transition. (b) The temperature dependence of the first-harmonic amplitude at ~ 29 T (i.e., above the kink) obtained by Fourier analysis of the dHvA data in this work (square symbols). A fit to the R_T factor $X/\sinh[X]$ (solid line; see text) gives an effective mass of $\sim 2.7 m_e$. The reanalyzed amplitudes of the SdH data at ~ 24 T of Ref. 4 are shown as diamond symbols for comparison; the fitted curve also gives an effective mass of $\sim 2.7 m_e$. All of the amplitudes are renormalized to 1.